[14] P. G. de Gennes, J. Prost, *The Physics of Liquid Crystals*, 2nd ed., Oxford University Press, New York **1993**.

[15] M. A. Unger, H. P. Chou, T. Thorsen, A. Sherer, S. R. Quake, *Science* **2000**, *288*, 113.

[16] J. P. Rolland, R. M. van Dam, D. A. Shorzman, S. R. Quake, J. M. DeSimone, *J. Am. Chem. Soc.* **2004**, *126*, 2322.

[17] A. I. Bishop, T. A. Nieminen, N. R. Heckenberg, H. Rubinsztein-Dunlop, *Phys. Rev. Lett.* **2004**, *92*, 198 104.

[18] Z. Cheng, T. G. Mason, *Phys. Rev. Lett.* **2003**, *90*, 018 304.

[19] A. La Porta, M. D. Wang, *Phys. Rev. Lett.* **2004**, *92*, 190 801.

[20] V. Garces-Chavez, D. McGloin, M. J. Padgett, W. Dultz, H. Schmitzer, K. Dholakia, *Phys. Rev. Lett.* **2003**, *91*, 093 602.

A Zone-Casting Technique for Device Fabrication of Field-Effect Transistors Based on Discotic Hexa-*peri*-hexabenzocoronene**

By *Wojciech Pisula, Anoop Menon, Michael Stepputat, Ingo Lieberwirth, Ute Kolb, Adam Tracz, Henning Sirringhaus, Tadeusz Pakula*, and *Klaus Müllen**

Organic semiconductors have attracted considerable interest over the last decade due to an immense improvement in the performance of electronic devices based on these materials. This attention has mainly been focused on conjugated polymers and oligomers, as well as small molecules which can be utilized as active layers in devices such as field-effect transistors (FETs),[1,2] photovoltaic cells,[3] and light-emitting diodes.[4] An interesting group of materials with potential application as organic semiconductors in electronic devices are columnar discotics.[5,6] These mesogens consist of an aromatic

[*] Prof. K. Müllen, W. Pisula, Dr. I. Lieberwirth, Prof. T. Pakula
Max-Planck-Institut für Polymerforschung
Ackermannweg 10, D-55128 Mainz (Germany)
E-mail: muellen@mpip-mainz.mpg.de

Dr. A. Menon, Prof. H. Sirringhaus
Plastic Logic Limited
34 Cambridge Science Park, Milton Road, Cambridge CB4 0FX (UK)

M. Stepputat, Dr. U. Kolb
Institut für Physikalische Chemie
Johannes Gutenberg-Universität Mainz
Welderweg 11, D-55099 Mainz (Germany)

Dr. A. Tracz
Center of Molecular and Macromolecular Studies
Polish Academy of Sciences
PL-90-363 Lodz, Sienkiewicza 112 (Poland)

core, which can be chemically modified by peripheral substitution (e.g., with alkyl chains), and self-assemble into one-dimensional (1D) columnar superstructures that then arrange in a two-dimensional (2D) lattice. The overlapping of the π orbitals of adjacent molecules within the columns ensures 1D intracolumnar charge-carrier transport. Another essential requirement for undisturbed 1D charge migration along the columns is a high degree of long-range order in the active layer which is deposited between the electrodes.[7] Local defects at domain boundaries in unoriented layers can trap charge carriers and significantly decrease the device performance.

Thus, the development of appropriate processing techniques became an essential challenge for the fabrication of unperturbed long-range-oriented organic semiconductors. This close relationship between supramolecular structure and electronic properties has been investigated impressively for planar metallophthalocyanine (Pc) and metalloporphyrin derivatives, in which the charge-carrier mobility of the holes depends strongly on the processing technique.[8–11] For vacuum-deposited thin layers of phthalocyanine, the mobility varied from 10^{-4} cm^2 V^{-1} s^{-1} for nickel Pc[8] to 0.02 cm^2 V^{-1} s^{-1} for copper Pc.[9,10] Other processing techniques, such as solution deposition onto substrates with a friction-oriented poly(tetrafluoroethylene) (PTFE) layer[12] and the Langmuir–Blodgett (LB) method, require chemical substitution of Pc, which results in decreased mobility in comparison to samples prepared by vacuum deposition.[13]
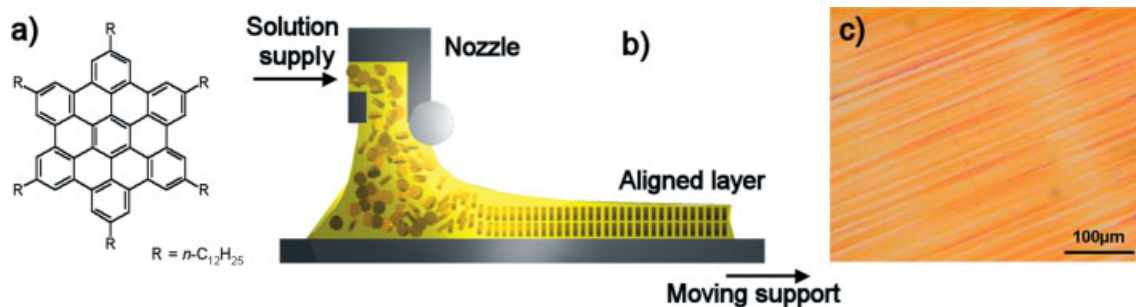
The history of discotic liquid-crystalline hexa-*peri*-hexabenzocoronene (HBC) derivatives as semiconductors is significantly shorter than that of phthalocyanines. Nevertheless, HBC derivatives have been successfully exploited in photovoltaic devices and field-effect transistors.[14] FETs were prepared by solution casting on substrates with the pre-oriented PTFE layer, resulting in uniaxial columnar order with an edge-on arrangement of the molecules.[15] The high supramolecular orientation was confirmed by field-effect anisotropy: the charge-carrier mobilities along the columns were significantly higher than in the perpendicular direction.[16] The high anisotropy of the charge-carrier mobility was demonstrated by flash-photolysis time-resolved microwave conductivity measurements.[17] The LB technique[18] and zone crystallization[19] have also been reported as efficient methods to obtain layers based on HBC derivatives, which are highly ordered over a long range.

Recently, we reported a novel orientation technique involving the zone-casting of dodecyl-substituted HBC (HBC-C$_{12}$, Fig. 1a,b) from solution directly onto a desired support.[20] Atomic force microscopy (AFM) studies revealed long-range order of the columnar structures uniaxially aligned in the casting direction. Due to the high order and unique molecular arrangement between the two phases, these layers also showed interesting optical properties.[21] The optical anisotropy of the HBC-C$_{12}$ layers was switched reversibly between two considerably different values: a negligibly low level in the crystalline phase at low temperatures, and a high level in the mesophase at higher temperatures.

Figure 1. a) Chemical structure of the dodecyl-substituted HBC derivative (HBC-C_{12}). b) Schematic presentation of the zone-casting technique. The continuously supplied solution is spread by means of a nozzle onto a moving support. The solution as well as the support are thermally controlled. Under appropriate rates of solvent evaporation and solution supply, a stationary gradient of concentration is formed within the meniscus. This results in directional crystallization. c) An optical microscopy image taken in reflection mode for a zone-cast HBC-C_{12} layer on a silicon substrate.

In this work, we employ the zone-casting method for the fabrication of long-range-oriented HBC-C_{12} films in order to attain highly ordered active layers in FETs. Both HBC-C_{12}, which is very attractive for potential applications in devices due to its high intrinsic charge-carrier mobility of up to 1.1 $cm^2 V^{-1} s^{-1}$, and the processing technique, which allows the fabrication of highly ordered layers over large areas, are of great interest in transistor applications.[22] Furthermore, we investigate the relationship between supramolecular organization revealed by structural analysis and charge-transport properties obtained from FET experiments.[30]

The morphology and structure of the zone-cast HBC-C_{12} thin layers are strongly dependent on the processing conditions. HBC-C_{12} drop-cast from solution forms long ribbons exceeding several micrometers in length, indicating strong aggregation in solution.[23] Due to this pronounced nucleation and growth ability, this compound appears to be a promising candidate for zone-cast processing. Under optimized zone-casting conditions, homogeneous films in the square-centimeter range on untreated glass, as well as on a hexamethyldisilazane (HMDS) modified silicon surface, were obtained, as shown by the optical microscopy image in Figure 1c. The hydrophobicity of the silicon surface was increased by HMDS modification in order to obtain a pronounced edge-on arrangement of the discotic molecules.[24] A film thickness of approximately 20 nm was determined.

High-resolution transmission electron microscopy (HRTEM) images, as presented in Figure 2, confirm the homogenous morphology of the HBC-C_{12} zone-cast film down to the nanometer scale. At higher

HRTEM magnifications, single columnar features appear along the casting direction with perfect columnar orientation, suggesting a high supramolecular order. The in-plane average intercolumnar distance of 2.48 nm was derived from the fast-Fourier-transform (FFT) pattern in Figure 2b, which also re-
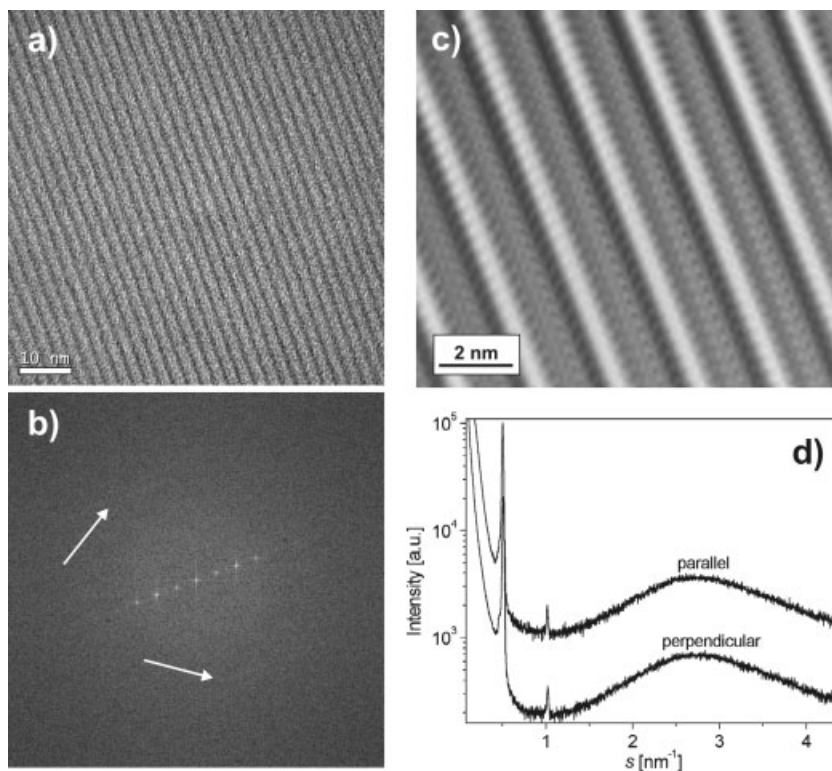

Figure 2. a) Large-area image from HRTEM of a zone-cast HBC-C_{12} layer displaying homogeneous film formation with single columnar features lying in the zone-casting direction. b) Fast-Fourier-transform (FFT) image confirming the structural order of columns, with an intercolumnar distance of 2.48 nm. The equatorial higher-order peaks indicate the pronounced columnar orientation. The intracolumnar stacking is represented by weak and diffuse meridional peaks (indicated by white arrows). c) Filtered inverse-FFT (IFFT) image showing the intermolecular periodicity within the columns. d) XRD pattern of zone-cast HBC-C_{12} measured parallel and perpendicular to the deposition direction. The scattering vector s is defined as $2 \sin \theta / \lambda$, where 2θ is the scattering angle and λ is the radiation wavelength.

http://www.advmat.de

vealed higher-order peaks emphasizing the long-range uniformity of columnar alignment in the casting direction, whereby the column length exceeded by far the investigated area. The intracolumnar stacking period of the discotic molecules of 0.49 nm was determined from low-intensity meridional peaks in the FFT pattern. Although these periodic features were very sensitive to the high-energy electron radiation, the filtered inverse-FFT image revealed an obvious intracolumnar periodicity corresponding to the stacking of the discs. From the fact that these columnar superstructures were formed by the self-assembly of the discotic molecules, an edge-on arrangement of the molecules was concluded. The columnar orientation visible in the HRTEM image in Figure 2a is very similar to the one visualized by means of AFM.[20] Taking into account that AFM gives information only about the surface and that HRTEM provides information about the "bulk" morphology of the thin layer, the similarity of the images obtained by these techniques is very important. Strong contrast in the HRTEM image, with a periodicity corresponding to the distance between the columns, proves that the columns in successive layers are positioned one on top of each other, correlating to a rectangular columnar packing. This conclusion is further supported by the X-ray- and electron-diffraction studies described below. On the other hand, since the intracolumnar periodicity is barely visible in the HRTEM image, the positions of the discotic molecules within adjacent columns cannot be strongly correlated. A converse molecular tilting angle in columns lying on top of one another might be a reason for the invisibility of these periodic features.

The high out-of-plane order was verified by X-ray diffraction (XRD) in reflection performed perpendicular to the casting direction, which displayed two characteristic reflections that were attributed to the out-of-plane periodicities of 1.98 nm. The high degree of order in this plane was emphasized by the appearance of the second-order peak at 1 nm^{-1}; this implied uniformity in the columnar structure, which was also reflected in the HRTEM results. Since the columnar axes were oriented parallel to the support, the disc-stacking periodicity along the columns did not appear in the XRD pattern performed parallel to the casting direction.

The electron-diffraction pattern shown in Figure 3 exhibits a pattern characteristic of a crystalline and highly ordered zone-cast HBC-C$_{12}$ layer at room temperature. Furthermore, this pattern includes essential information about all the characteristic in-plane and inter- and intracolumnar periodicities. The regular columnar organization, with a repeat distance of 2.48 nm seen in the HRTEM image, was also evident as the first peak in the equatorial-reflection distribution, assigned as the (h00) plane. Since the columnar arrangement corresponds to a herringbone structure, the (100) reflection, being double the value of the simple in-plane intercolumnar distance, was not displayed. The assumption of the absence of this peak, corresponding to a periodicity of 4.96 nm, was verified when the positions of the equatorial reflections were fitted to a mathematical relation assigning these reflections to one packing parameter of a 2D unit cell. The significant difference in
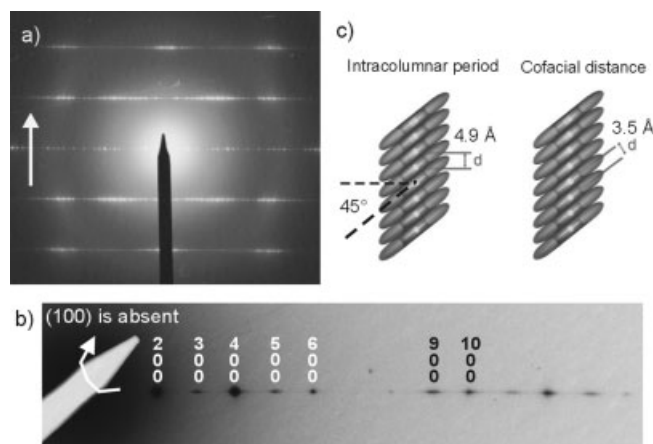
Figure 3. a) Electron-diffraction pattern of a zone-cast HBC-C$_{12}$ layer (white arrow indicating the casting direction). b) Schematic representation of the intracolumnar arrangement. Discotic molecules show a molecular tilting of 45°, which gives two characteristic reflections corresponding to the intracolumnar period and the cofacial distance between two adjacent discs. c) Assignment of the equatorially distributed reflections indicating the in-plane intercolumnar order by using Miller indices (hkl).

intensity between the odd and even (h00) reflections emphasized the relation of adjacent columns with discs of different tilt (herringbone structure).[25] The resulting tilt angle of the molecules was calculated from the reflections with maximum intensity in the (h01) line. The determined angle was approximately 45° towards the columnar axis with a rotation axis perpendicular to the support. The high structural intra- and intercolumnar order as well as the exact disc tilt of 45° were responsible for the reported switching of the optical anisotropy of the film between the crystalline phase and the mesophase.[21] The characteristic cofacial distance of 0.34 nm is related to the maximum intensity of the (h01) reflections, whereas the intracolumnar period of 0.49 nm corresponds to the positions of the reflection lines. By combining data from both the X-ray and electron-scattering techniques, an orthorhombic unit cell consisting of tilted HBC-C$_{12}$ molecules in the crystalline phase was identified, as presented schematically in Figure 4. The small out-of-plane correlation distance can be explained by an irregular distribution of the alkyl chains at
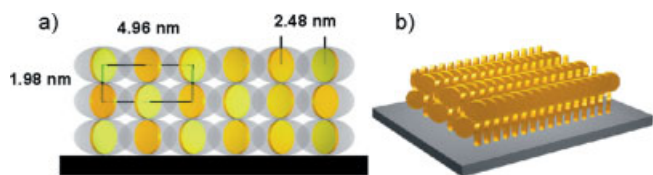
Figure 4. a) Primary schematic presentation of a cross-section of a zone-cast HBC-C$_{12}$ layer. The 2D lateral orthorhombic unit-cell assignment of the HBC-C$_{12}$ columnar arrangement in the crystalline phase is based on TEM and XRD results (the aromatic core is represented as a disc and the side chains are shown schematically as the surrounding translucent ellipsoids). b) Schematic drawing of the columnar orientation with edge-on arrangement of the tilted HBC-C$_{12}$ molecules on the support.

the core periphery. It should be noted that the proposed unit-cell assignment is tentative because of the limits of both the techniques used in this study. However, the unit-cell parameters determined by this structure investigation are significantly smaller than those found for the lattice in bulk samples.[26] This significant difference in packing parameters might result from enhanced packing of the columns in the zone-cast film. An additional reason is an improved peripheral organization of the alkyl chains and a slightly different tilt angle of the discs. A molecular tilt angle of approximately 30° was determined for the sample in the bulk. The significant decrease in unit-cell parameters, the pronounced columnar orientation, and the appearance of the characteristic intracolumnar correlation of 0.35 nm can be regarded as consequences of the refined packing of the discotic molecules, resulting in improved charge-carrier migration due to enhanced overlap of the π orbitals.[27]

The most important application of the zone-casting technique in the case of HBC-C$_{12}$ is considered to be the fabrication of a highly aligned semiconductor layer in the channel of an FET. The uniaxially aligned HBC-C$_{12}$ thin surface layer in the channel of the FET should enhance device performance as an active component. In order to demonstrate this, FETs were fabricated on top of a SiO$_2$ insulating layer on a silicon substrate by direct zone-casting. The device was constructed with top contacts having a channel length of 25 μm between the shadow-masked source and drain gold electrodes. A schematic drawing of the device design is shown in Figure 5a. The transfer and output characteristics of the devices measured parallel to the columnar alignment are shown in Figures 5b,c, revealing a very good on–off ratio of 10^4, a high field-effect mobility in the saturation regime at 5×10^{-3} cm^2 V^{-1} s^{-1}, and a turn-on voltage of ca. –15 V. In some devices, a mobility as high as 1×10^{-2} cm^2 V^{-1} s^{-1} was also observed. In previously reported data by van de Craats et al.,[16] it was found that the highest achievable mobility of an oriented HBC derivative on an aligned PTFE layer on silicon was 0.5×10^{-3} cm^2 V^{-1} s^{-1}. The device dimensions reported there were similar to the current case. We have demonstrated an order-of-magnitude improvement in the device on-currents (I_{on}) and the saturation mobility by zone-casting the discotic semiconductor system. The superior device performance is attributed to the highly ordered and uniformly oriented HBC-C$_{12}$ that can be realized by the zone-casting technique. However, it should be noted that the charge-carrier mobilities of HBC-C$_{12}$ exposed in FETs are still two orders of magnitude lower than the intrinsic values obtained by pulse-radiolysis time-resolved microwave conductivity. One reason for this considerable difference concerns possible contact problems between the drain and source and the active organic layer. Another contributing factor could be related to the presence of local intracolumnar packing defects, which can constitute localized barriers for charge-carrier movement along the columns. Even at low concentrations, these defects can significantly decrease charge-carrier transport over longer distances. The inversion of a filtered
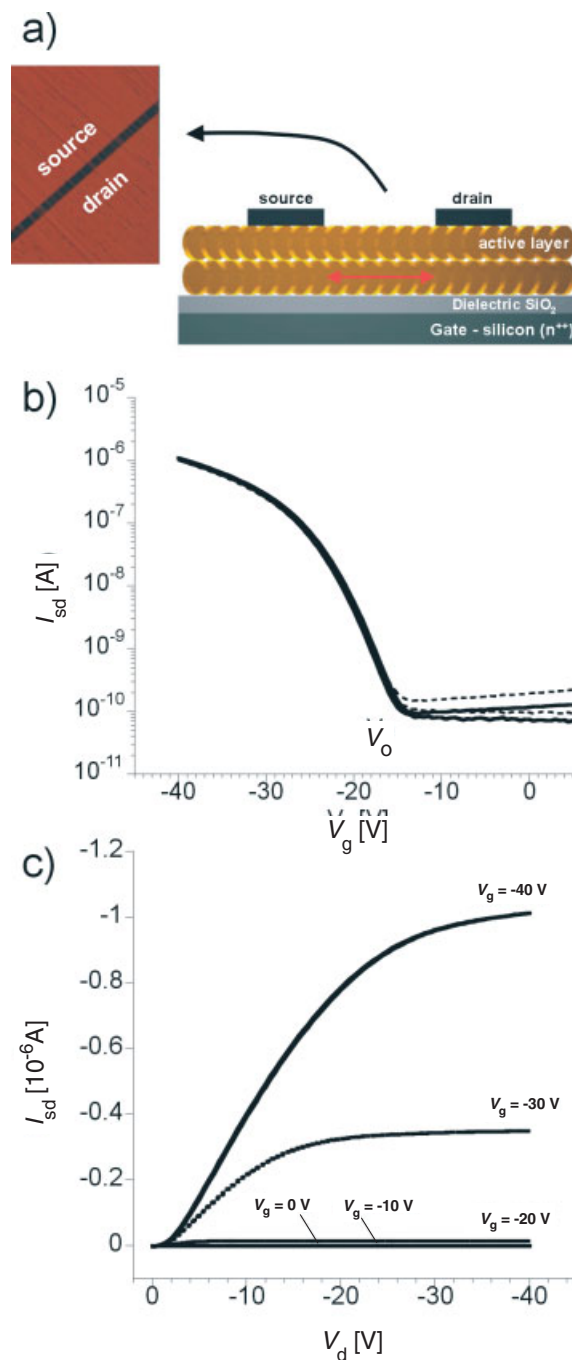
Figure 5. a) Schematic side-view representation of the top-contact device configuration with contacts evaporated (channel length $L = 25$ mm, width $W = 1.6$ mm, and depth $d = 200$ nm) onto the 20 nm thick zone-cast HBC-C$_{12}$ aligned film. A 200 nm SiO$_2$ dielectric and an n-doped silicon substrate as a gate electrode were used in this device configuration. The discs represent the tilted molecules in edge-on arrangement. The red arrow indicates the charge-transport direction. The optical image shows the aligned layer in a 25 μm long channel of an FET. b) Typical transfer characteristics (gate voltage $V_g = -40$ V) of an FET with zone-cast HBC-C$_{12}$ as an active layer. The mobilities were extracted from the saturation régime by conventional techniques. c) Current–voltage (I–V) output characteristics. Both dependencies are measured along the columnar alignment. V_d: drain voltage; I_{sd}: source–drain current.

FFT image, shown in Figure 6, indeed reveals single defects in the intracolumnar order. One could also conclude that these defects were not limited to one plane, but progressed three-dimensionally.
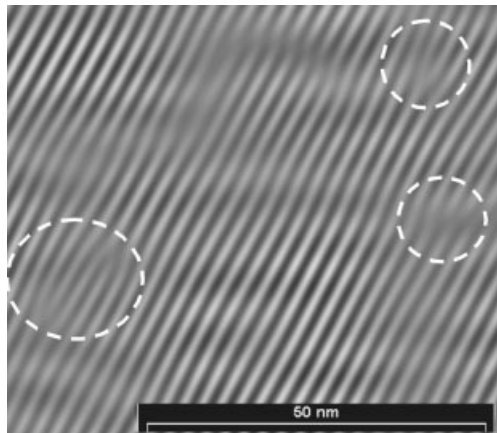
Figure 6. Filtered IFFT of an electron microscopy image of zone-cast HBC-C_{12}. Dashed circles indicate the intracolumnar defects.

Although these defects appeared sporadically, charge-carrier transport might be influenced significantly over long ranges between the electrodes. On the other hand, the presence of local defects, for example, even in organic single crystals, is extremely difficult to control by any processing technique. The device characteristics of HBC-C_{12} approach those of state-of-the-art organic semiconductors such as dioctylfluorene–bithiophene copolymers by virtue of the highly ordered zone-cast films.[28] In order to exploit these materials in applications such as active-matrix backplanes, further studies are required into stress and environmental stability.

In summary, we have demonstrated that zone casting is a powerful technique for fabricating FETs based on highly oriented HBC-C_{12}. The device performance reported in this work is at least an order of magnitude higher than previously reported values. Thus, the zone-casting technique opens new pathways for fabricating large-scale thin layers of highly oriented semiconductors and enhancing the charge transport within the existing process at room temperature. This is an important step towards improving the performance of organic semiconductors in electronic devices.

Experimental

The synthesis of dodecyl-substituted hexa-*peri*-hexabenzocoronene (HBC-C_{12}) was performed according to a procedure reported elsewhere [29]. Oriented layers of HBC-C_{12} on hexamethyldisilazane (HMDS) treated silicon dioxide (SiO_2) were obtained by means of the zone-casting technology using a specially constructed device. For the zone-cast procedure, HBC-C_{12} was dissolved in tetrahydrofuran (THF) at a concentration of 0.25 mg mL^{-1}. The fabrication took place in ambient atmosphere. The solvent temperature was 51 °C and the support temperature was 46 °C. The support velocity was 35 μm s^{-1}.

By using 1 mL of the solvent with the above-mentioned concentration, it was possible to cover an area of more than 12 cm^2 with a homogeneous aligned film.

Optical images of the films were taken using a Hitachi KP-D50 Color Digital charge-coupled device (CCD) camera on a Zeiss microscope equipped with polarizing filters.

High-resolution transmission electron microscopy (HRTEM) was carried out on a FEI Tecnai F30 ST at 300 kV under liquid N_2 cryoconditions. Electron diffraction was recorded using a Philips CM 12 electron microscope at 120 kV acceleration voltage. In both cases, the films were first cast onto a carbon film evaporated onto a glass substrate. Then, the HBC-C_{12}/carbon film was removed from the glass using a dilute aqueous HF solution and carefully mounted onto a TEM copper grid.

X-ray diffraction was performed on a θ–θ Philips PW 1820 Kristalloflex diffractometer with a graphite-monochromatized Cu Kα X-ray beam incident on a zone-cast HBC-C_{12} film on a pure glass substrate, at room temperature, in both casting directions (parallel and perpendicular).

For the preparation of HMDS-treated Si(n^{++})/SiO_2 wafers, the substrates were plasma-cleaned in an oxygen plasma for 30 s. After this, the HMDS was spin-cast at 2000 revolutions per minute (rpm) on the substrate, followed by a 30 min bake at 100 °C. Field-effect transistors were fabricated by zone casting HBC-C_{12} on an HMDS-treated Si(n^{++})/SiO_2 wafer using the procedure described earlier. Source–drain contacts were made on top of the HBC-C_{12} films by shadow-mask evaporation, yielding a channel length of 25 μm and a width of 1.6 mm. The gate dielectric was SiO_2 with a thickness of 200 nm. All device characteristics were measured at room temperature with a semiconductor parameter analyzer HP 4155B in a glove box and under a dry nitrogen atmosphere ($H_2O < 1$ ppm, $O_2 < 5$ ppm).

[1] C. D. Dimitrakopoulos, P. R. L. Malenfant, *Adv. Mater.* **2002**, *14*, 99.

[2] G. Horowitz, *Adv. Mater.* **1998**, *10*, 365.

[3] C. J. Brabec, N. S. Sariciftci, J. C. Hummelen, *Adv. Funct. Mater.* **2001**, *11*, 15.

[4] M. O'Neill, M. Kelly, *Adv. Mater.* **2003**, *15*, 1135.

[5] D. Adam, P. Schuhmacher, J. Simmerer, L. Haussling, K. Siemensmeyer, K. H. Etzbach, H. Ringsdorf, D. Haarer, *Nature* **1994**, *371*, 141.

[6] N. Boden, R. J. Bushby, J. Clements, B. Movaghar, K. J. Donovan, T. Kreouzis, *Phys. Rev. B*: *Condens. Matter Mater. Phys.* **1995**, *52*, 13 274.

[7] V. Lemaur, D. A. da Silva Filho, V. Coropceanu, M. Lehmann, Y. Geerts, J. Piris, M. G. Debije, A. M. van de Craats, K. Senthilkumar, L. D. A. Siebbeles, J. M. Warman, J.-L. Brédas, J. Cornil, *J. Am. Chem. Soc.* **2004**, *126*, 3271.

[8] G. Guillaud, J. Simon, *Chem. Phys. Lett.* **1994**, *219*, 123.

[9] Z. Bao, A. J. Lovinger, A. Dodabalapur, *Appl. Phys. Lett.* **1996**, *69*, 3066.

[10] Z. N. Bao, A. J. Lovinger, A. Dodabalapur, *Adv. Mater.* **1997**, *9*, 42.

[11] Y.-Y. Noh, J.-J. Kim, Y. Yoshida, K. Yase, *Adv. Mater.* **2003**, *15*, 699.

[12] X. L. Chen, A. J. Lovinger, Z. Bao, J. Sapjeta, *Chem. Mater.* **2001**, *13*, 1341.

[13] J. Locklin, K. Shinbo, K. Onishi, F. Kaneko, Z. N. Bao, R. C. Advincula, *Chem. Mater.* **2003**, *15*, 1404.

[14] L. Schmidt-Mende, A. Fechtenkotter, K. Müllen, E. Moons, R. H. Friend, J. D. MacKenzie, *Science* **2001**, *293*, 1119.

[15] O. Bunk, M. M. Nielsen, T. I. Solling, A. M. van de Craats, N. Stutzmann, *J. Am. Chem. Soc.* **2003**, *125*, 2252.

[16] A. M. van de Craats, N. Stutzmann, O. Bunk, M. M. Nielsen, M. Watson, K. Müllen, H. D. Chanzy, H. Sirringhaus, R. H. Friend, *Adv. Mater.* **2003**, *15*, 495.

[17] J. Piris, M. G. Debije, N. Stutzmann, A. M. van de Craats, M. D. Watson, K. Müllen, J. M. Warman, *Adv. Mater.* **2003**, *15*, 1736.

[18] N. Reitzel, T. Hassenkam, K. Balashev, T. R. Jensen, P. B. Howes, K. Kjaer, A. Fechtenkotter, N. Tchebotareva, S. Ito, K. Müllen, T. Bjornholm, *Chem. Eur. J.* **2001**, *7*, 4894.

[19] W. Pisula, M. Kastler, D. Wasserfallen, T. Pakula, K. Müllen, *J. Am. Chem. Soc.* **2004**, *126*, 8074.

[20] A. Tracz, J. K. Jeszka, M. D. Watson, W. Pisula, K. Müllen, T. Pakula, *J. Am. Chem. Soc.* **2003**, *125*, 1682.

[21] J. Piris, W. Pisula, A. Tracz, T. Pakula, K. Müllen, J. Warman, *Liq. Cryst.* **2004**, *31*, 993.

[22] A. M. van de Craats, J. M. Warman, *Adv. Mater.* **2001**, *13*, 130.

[23] A. Tracz, D. Wostek, I. Kucinska, J. K. Jeszka, M. Watson, K. Müllen, T. Pakula, in *Molecular Low Dimensional and Nanostructured Materials for Advanced Applications* (Eds: A. Graja, R. Bulka, F. Kajzar), Kluwer, Dordrecht, The Netherlands **2002**, p. 315.

[24] R. A. P. Zangmeister, P. E. Smolenyak, A. S. Drager, D. F. O'Brien, N. R. Armstrong, *Langmuir* **2001**, *17*, 7071.

[25] R. Goddard, M. W. Haenel, W. C. Herndon, C. Kriiger, M. Zander, *J. Am. Chem. Soc.* **1995**, *117*, 30.

[26] I. Fischbach, T. Pakula, P. Minkin, A. Fechtenkotter, K. Müllen, H. W. Spiess, K. Saalwachter, *J. Phys. Chem. B* **2002**, *106*, 6408.

[27] M. D. Curtis, J. Cao, J. W. Kampf, *J. Am. Chem. Soc.* **2004**, *126*, 4318.

[28] H. Sirringhaus, R. J. Wilson, R. H. Friend, M. Inbasekaran, W. Wu, E. P. Woo, M. Grell, D. D. C. Bradley, *Appl. Phys. Lett.* **2000**, *77*, 406.

[29] A. Stabel, P. Herwig, K. Müllen, J. P. Rabe, *Angew. Chem. Int. Ed. Engl.* **1995**, *34*, 1609.

[30] P. Miskiewicz, J. Ulanski, the first field-effect observations for zone-cast discotics were made in the group of Prof. Ulanski, Department of Molecular Physics, Techniual University of Lodz, Poland, unpublished results.

Encapsulation of Catalysts in Supramolecular Porous Frameworks: Size- and Shape-Selective Catalytic Oxidation of Phenols**

By *Ling-Guang Qiu,* *An-Jian Xie,* and *Li-De Zhang*

Catalysis is known to play a key role in modern chemical technology, and zeolites are among the most important catalysts used on a large scale in the chemical industry because of their inherent capability of product selectivity. Zeolites in whose matrix cavities transition metal complexes are encapsulated can exhibit the engineering advantages of solid heterogeneous catalysts, such as easy separation, ruggedness, high-selectivity, etc., and yet have many of the advantageous features of homogeneous catalysts.[1–7] There are two main approaches to their production, namely, the zeolite synthesis (ZS) and flexible ligand (FL) methods. In the ZS method, however, the metal complexes can decompose under the conditions of zeolite synthesis, such as high pH and elevated temperatures. In addition, poor solubility of the complexes in the synthesis medium can result in a low content of the metal complexes in the final product. In the FL method, a flexible ligand, which is able to diffuse freely through the zeolite pores, complexes with a previously exchanged metal ion. The procedure of encapsulation is very complicated: the amount of ligand should be greatly in excess of the metal ions (the product must be extracted using large quantities of solvent until all the unreacted ligand is removed) while, at the same time, too large a quantity of metal complexes should not be encapsulated in the zeolites, as this may result in pore blockage.[3–7]

Recently, there has been a surge of research interest in metal–organic frameworks (MOFs), because of their potential applications in catalysis, photonics, separation, gas storage, and molecular sensing.[8–12] Compared to traditional zeolites and recently developed MCM-type mesoporous materials, MOFs are synthesized under mild conditions and allow systematic engineering of their chemical and physical properties through modification of their components (seminal work by Robson et al.[13] and a systematical study by Yaghi et al.[14] have clearly established the feasibility of designing porous solids with precisely controlled pore size and chemical functionality). However, it has been difficult to construct catalytically active MOFs, because the metal ion and the ligand are usually selected as building blocks of the MOFs rather than as catalysts. As a result, most MOFs have no potential catalytic activity, and few catalytically active MOFs have been exploited until now.[15–17] Given that zeolites that have metal complexes encapsulated in their matrix cavities possess the advantages of solid heterogeneous catalysts, we consider whether it is possible to encapsulate metal complexes into MOFs through supramolecular self-assembly.

Herein, we chose two simple building units, 1,3,5-benzenetricarboxylate (BTC) and the hexaaquo metal complexes $[M(H_2O)_6]^{2+}$ (M = Mn or Cu), to illustrate the strategy of encapsulating the metal complex $[Mn(phen)_2(H_2O)_2]^{2+}$ (phen = 1,10-phenanthroline) into supramolecular frameworks through hydrogen bonding and π–π interactions. Excellent size- and shape-selective catalytic activity of these supramolecular frameworks in the oxidation of phenols will be presented.

An aqueous solution of Na₃BTC and a mixed solution of MnCl₂ and *cis*-[Mn(phen)₂]Cl₂ were allowed to diffuse slowly in a U-shaped tube across an agar-gel medium at 2 °C, to yield cubic, light-yellow crystals of $[Mn^{II}(H_2O)_6] \cdot [Mn^{II}(phen)_2(H_2O)_2]_2 \cdot 2BTC \cdot 24H_2O$ (**1**). When CuCl₂·6H₂O was used instead of MnCl₂, a mixed-metal, three-dimensional (3D), hydrogen-bonded framework $[Cu^{II}(H_2O)_6] \cdot [Mn^{II}(phen)_2(H_2O)_2]_2 \cdot 2BTC \cdot 22H_2O$ (**2**) formed. X-ray structural analy-

[*] Dr. L.-G. Qiu, Prof. L.-D. Zhang
Institute of Solid State Physics
Chinese Academy of Sciences
Hefei 230 031 (P.R. China)
E-mail: lgqiu.issp@163.com
Dr. L.-G. Qiu
School of Chemistry and Chemical Engineering
Anhui University
Hefei 230 039 (P.R. China)
Prof. A.-J. Xie
School of Chemistry and Chemical Engineering
Anhui University
Hefei 230039 (P.R. China)

© 2005 WILEY-VCH Verlag GmbH & Co. KGaA, Weinheim